# *A structural modeling approach for the understanding of initiation and elongation of ALS-linked superoxide dismutase fibrils*

**Mattia Falconi, Federico Iacovelli & Alessandro Desideri**

**Journal of Molecular Modeling**
Computational Chemistry - Life Science - Advanced Materials - New Methods

ISSN 1610-2940

J Mol Model
DOI 10.1007/s00894-013-1896-7

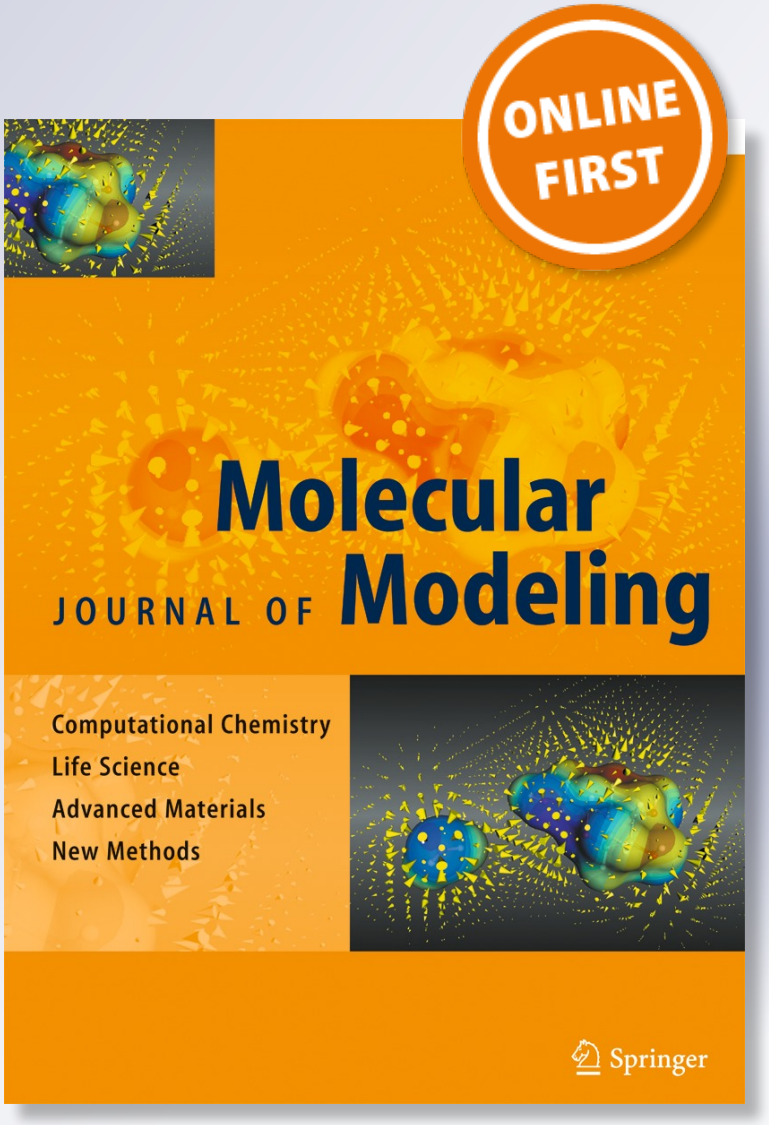


Springer

J Mol Model
DOI 10.1007/s00894-013-1896-7

ORIGINAL PAPER

# A structural modeling approach for the understanding of initiation and elongation of ALS-linked superoxide dismutase fibrils

**Mattia Falconi · Federico Iacovelli · Alessandro Desideri**

Received: 27 February 2013 / Accepted: 23 May 2013


**Abstract** Familial amyotrophic lateral sclerosis caused by mutations in copper-zinc superoxide dismutase (SOD1) is characterized by the presence of SOD1-rich inclusions in spinal cords. It has been shown that a reduced intra-subunit disulfide bridge apo-SOD1 can rapidly initiate fibrillation forming an inter-subunits disulfide under mild, physiologically accessible conditions. Once initiated, elongation can proceed via recruitment of either apo or partially metallated disulfide-intact SOD1 and the presence of copper, but not zinc, ions inhibit fibrillation. We propose a structural model, refined through molecular dynamics simulations, that, taking into account these experimental findings, provides a molecular explanation for the initiation and the elongation of SOD1 fibrils in physiological conditions. The model indicates the occurrence of a new dimeric unit, prone to interact one with the other due to the presence of a wide hydrophobic surface and specific electrostatic interactions. The model has dimensions consistent with the SOD1 fibril size observed through electron microscopy and provides a structural basis for the understanding of SOD1 fibrillation.

**Keywords** Amyotrophic lateral sclerosis · Cu,Zn superoxide dismutase · Fibrillation · Molecular dynamics simulation · Molecular modeling · Protein aggregation

**Electronic supplementary material** The online version of this article (doi:10.1007/s00894-013-1896-7) contains supplementary material, which is available to authorized users.

M. Falconi (✉) · F. Iacovelli · A. Desideri
Department of Biology, University of Rome "Tor Vergata", Via della Ricerca Scientifica,
00133 Rome, Italy
e-mail: falconi@uniroma2.it

M. Falconi · F. Iacovelli · A. Desideri
Interuniversity Consortium, National Institute Biostructure and Biosystem (INBB), Rome, Italy

## Introduction

Amyotrophic lateral sclerosis (ALS), known also as Lou Gehrig's disease, is a neurodegenerative disorder characterized by the destruction of large motor neurons in the spinal cord and brain. The disease results in progressive paralysis, usually culminating in death within 2–5 years after the onset of symptoms [1]. Of all ALS cases, <10 % are familial, and <20 % of these familial ALS (fALS) cases are associated with dominantly inherited mutations in copper-zinc superoxide dismutase (SOD1) [2, 3].

The dimeric metallo-protein SOD1 is a β-rich, antioxidant enzyme, abundantly present in the cytoplasm, in which each subunit of the mature form, composed of 153 residues, contains a copper and a zinc ion and an intra-chain disulfide bond [4]. In vitro studies have shown that the presence of the copper and zinc metal cofactors protect the disulfide bond from reduction, suggesting an explanation for the persistence of the disulfide bond in the reducing environment of the cytoplasm [5]. More than 165 mutations in SOD1 have been identified in cases of fALS (http://alsod.iop.kcl.ac.uk/default.aspx).

Mutations in SOD1 that have been identified in fALS patients occur in 74 positions that are well dispersed over the length of this 153 residues polypeptide [6]. Previous studies suggest also that aggregates, composed in part of fALS SOD1, play a role in pathogenesis either by sequestering heat-shock proteins and molecular chaperones [7, 8], or by interfering with the neuronal axonal transport [9, 10] and protein degradation machineries [11]. Proteinaceous aggregates have been found in the spinal cords of ALS patients, and immuno-microscopy has confirmed that the protein inclusions, present in the spinal cords of SOD1-fALS patients, are rich in SOD1 [12, 13]. Bound copper and zinc, the intra-subunit disulfide bond and the dimeric nature of the protein all contribute to the unusually high stability of mature SOD1 [14]. The absence of one or more of these post-translational modifications may destabilize the structure of SOD1

Published online: 19 June 2013

sufficiently to allow misfolding into an amyloid form [14]. Previous studies have demonstrated that apo (metal free) SOD1 can be induced to form insoluble, fibrillar structures, but only under destabilizing conditions such as low pH [15], elevated temperature, presence of trifluoroethanol [16], or removal of the intra-subunit disulfide bond by mutation [17]. It is now generally accepted that the common effect of ALS-causing SOD1 mutations must involve an increase in the propensity for SOD1 to misfold and to aggregate, though until recently, the molecular details of these processes remained obscure [18–20]. To overcome the interpretation limits due to the static structures of the wildtype SOD1 and FALS mutants, Strange and coworkers [21] firstly simulate the human SOD1 enzyme through the molecular dynamics (MD) technique to reveal the first stages of misfolding caused by the metal depletion. In their simulation large spatial and temporal fluctuations of the active site loops, shaping the metal-binding sites, expose the dimer β-barrels to the external environment, allowing interactions with adjacent molecules. In addition they show that protection of the protein β-edge can be partially restored by incorporating a single Zn ion per dimer [21]. Using the same simulative technique, Ding and collaborators [22] study the structural dynamics of SOD1 monomer and dimer, with and without metal binding and under disulfide-intact or disulfide reduced environments, providing dynamical evidence to the stabilizing role of metal ions in both dimer and monomer SOD1. Furthermore, they show that the reduction of the disulfide bond in SOD1, with metal ions depleted, results in a flexible Glu49-Asn53 loop which disrupts the dimer formation [22]. In a subsequent work [23] atomistic MD simulations have been carried out to study the conformational dynamics of apoSOD1 monomer while coarse-grained MD simulations have been applied to study the aggregation of partially unfolded SOD1 monomers of wildtype SOD1 and two FALS mutants (G37R, and I149T). The obtained results support the hypothesis that the formation of aggregation "building blocks", achieved through apo-monomer local unfolding, represent the mechanism by which the SOD1 fibrillar aggregation may take place [23]. Experimentally it has been reported that small amounts of disulfide reduced, metal-free, monomeric SOD1 can rapidly initiate fibril formation in disulfide-intact forms of SOD1 under mild, physiologically relevant conditions [14]. Once initiated, SOD1 amyloid fibrils elongate by recruiting apo or partially metallated, dimeric, disulfide-intact SOD1. Moreover it has been shown that, once disulfide-reduced mutant SOD1 initiate fibrillation, wild type SOD1 can participate in the etiology of ALS [14].

Considering these results here we propose atomistic models that, taking into account the results obtained by the simulations [21–23] and the findings of Valentine and coworkers [14], show how the occurrence of an inter-subunits disulfide bridge may produce an altered dimer able to generate, through specific hydrophobic and electrostatic interactions, extended filamentous assemblies.

## Methods

### Molecular modeling

Three protein models have been built in order to structurally design the fALS fibril, i.e., a nucleation SOD1 dimer with a novel interface between the subunits, a dimer of dimers generated by two novel SOD1 assemblies and a hybrid tetramer. The modeling procedures have been executed through the SYBYL 6.0 software (Tripos Inc. 1699, South Hanley Road St. Louis, Missouri, 63144, USA). All the obtained structures have been preliminary checked against steric hindrance and then minimized. All the initial minimizations have been carried out in vacuum using SYBYL 6.0, imposing a max of 20 steps of the SIMPLEX algorithm and 500 steps of the Powell method, including all the hydrogen atoms and using the AMBER7_F99 force field (Tripos Inc. 1699, South Hanley Road St. Louis, Missouri, 63144, USA). The accurate positioning of the interface residues has been executed through the MD simulation refinement approach.

### A novel SOD1 dimer assembly: the disulfide linked dimer

The NMR structure of disulfide bridge reduced and copper depleted human SOD1 (PDB code: 2AF2) [24], has been utilized to generate a model of the putative nucleation dimer of the fALS fibril. The mutations present in the structure (i.e., Cys6Ala and Cys111Ser) have been reverted to cysteine residues. Among the 30 models, contained in the PDB file with code 2AF2, the fifth, displaying conformational features compatible with the modeling, i.e., with an ideal loop 6,5 conformation, has been chosen. The new dimer has been obtained translating from the original position (Fig. 1a) one SOD1 monomer and generating an inter-subunit disulfide bridge between the Cys57 belonging to the two monomers (Fig. 1b). The new dimer interface is mainly constituted by the two loops 6,5 with the Cys57 disulfide bridge in the center (Fig. 1b). In the disulfide linked SOD1 dimer assembly the hydrophobic interface, that stabilizes the standard quaternary structure of Cu,Zn SOD1, remains exposed to solvent (Fig. 1b) and has been used to model the interactions stabilizing higher order aggregates.

### The dimer of dimers

In order to reproduce the orientation of the original interface, one subunit of the novel dimer (Fig. 2a, blue) and one subunit of the standard dimer (Fig. 2a, green), have been transiently superimposed (Fig. 2b). After, a subunit of another novel

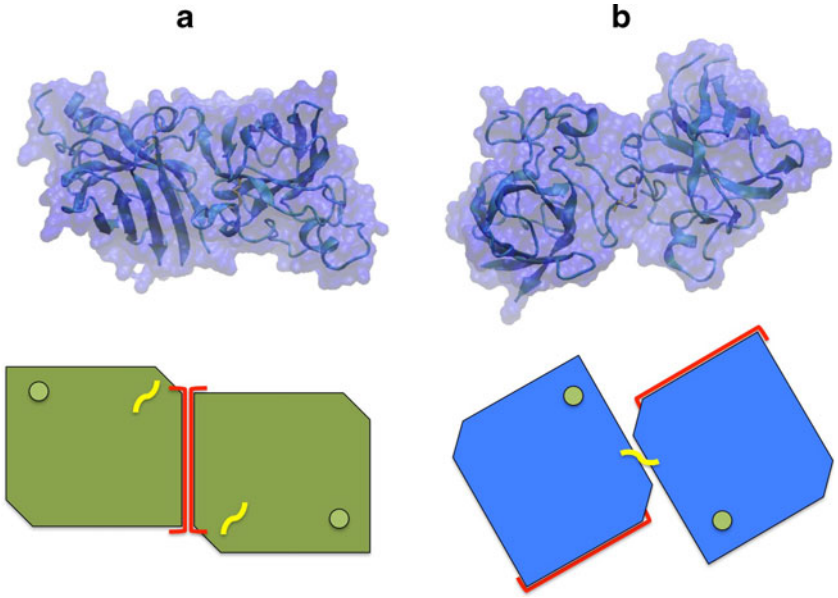


**Fig. 1** Ribbon (*top*) and schematic (*bottom*) representations of (**a**) the standard SOD1 dimer and (**b**) the inter-subunits disulfide linked SOD1 dimer. The SOD1 monomer is represented as a poligon, the *yellow bold line* indicates the position of the disulfide bridge, the *green circle* the zinc ion and the *red line* the location of the standard interface. The PyMOL [43] (http://www.pymol.org) program has been used to generate the top protein images shown in this picture

dimer has been superimposed on the remaining subunit of the standard SOD1 (Fig. 2c). Finally, removing the standard SOD1 dimer (Fig. 2d), two inter-subunit linked SOD1 dimers are coupled and, taking advantage of the original interface, generate the dimer of dimers. The obtained assembly maintains two standard hydrophobic interfaces that, being solvent exposed, become available for the fibril propagation.

## The hybrid tetramer

Starting from the dimer of dimers a hybrid tetramer structure has been modeled replacing one novel dimer with two standard SOD1 monomers with intra-subunit disulfide bridge, but without the copper ion, obtained from the PDB file 1HL4, using chains A and B [25].

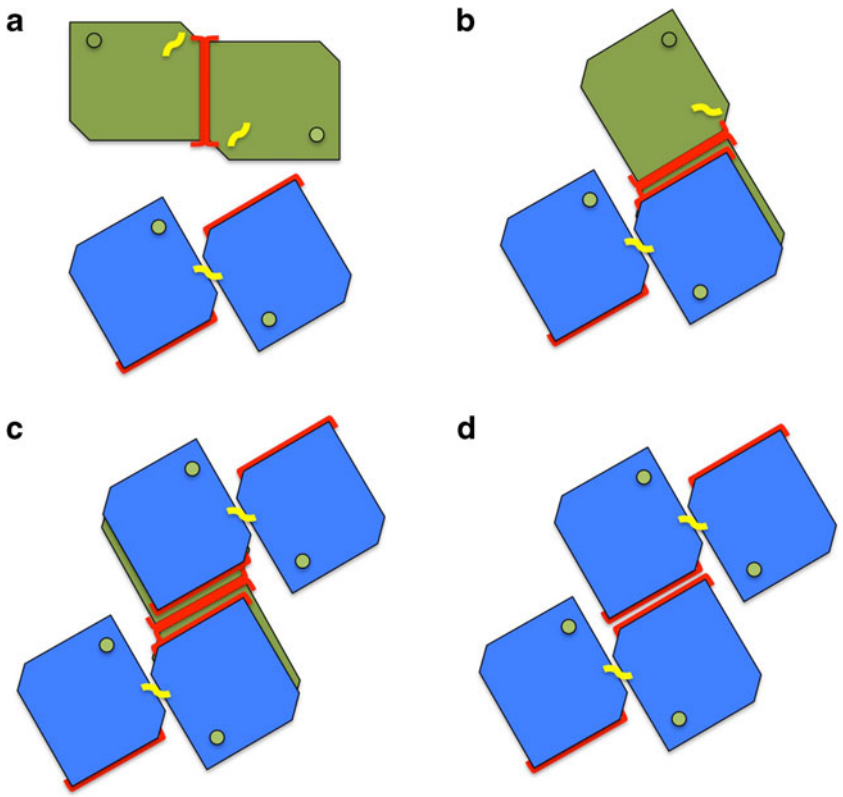


**Fig. 2** Scheme of the procedure used to build the ALS-linked SOD1 dimer of dimers. **a** Schematic representation of the standard SOD1 dimer (*green*) and of the inter-subunits disulfide linked dimer (*blue*). **b** Superposition of one subunit of the standard SOD1 dimer on one subunit of the first disulfide linked dimer. **c** Superposition of the other subunit of the standard SOD1 dimer on one subunit of a second inter-subunit disulfide linked dimer. **d** Removal of the standard SOD1 dimer and final assembly of the ALS-linked SOD1 dimer of dimers having the original standard dimer interface in the middle of the new extended interface

## Molecular dynamics simulations

The MD simulation technique has been used to refine the new interfaces formed in the fibril modeling steps and, representing a form of structural validation, certifies the reliability of the carried out modeling procedure. The system topologies have been obtained with the AMBER 12.0 [26] tleap module and modeled with the all-atoms AMBER03 force field [27]. The zinc ion has been parameterized through the cationic dummy atom approach (CaDa) [28]. The CaDA approach has been implemented in the AMBER03 force field [27] and has been applied to proteins containing Zn ions mainly coordinated by histidines and aspartic or glutammic acids [29] similar to the zinc coordination in SOD1. In detail the CaDA parameterization replaces the zinc divalent cation (one-atom representation) with the tetrahedron-shaped zinc divalent cation, composed of four dummy atoms (each one representing one Zn orbital) attached to the central zinc ion, deprotonating the zinc ligands and using histidinate for histidine. These aspects make the CaDA approach particularly appropriate for these MD simulations.

The three models have been immersed in a cubic box filled with TIP3P water molecules [30], imposing a minimal distance between the solute and the box walls of 10.0 Å. The systems have been neutralized through the AMBER [26] tleap module, adding the counterions (14 $Na^+$ ions for the dimer and 28 for the two dimers of dimers) in electrostatic favorable positions. Optimization and relaxation of the entire systems were initially performed through energy minimization of the solvent, ions and solute. After three MD runs, each 200 ps long, at 100, 200, and 300 K have been carried out to equilibrate the structures. The systems have been simulated in periodic boundary conditions, using a cut-off of 10 Å for the evaluation of short-range non-bonded interactions and the PME method for the long-range electrostatic interactions [31]. The SHAKE [32] and SETTLE [33] algorithms were used to constrain all bond lengths, for the protein and water, respectively. The temperature has been fixed at 300 K using the Langevin dynamics [34], whereas pressure has been held constant at 1 atm through the Langevin piston method [35]. The three models have been simulated for a total of 10 ns using the NAMD 2.9 MD package [36] and the atomic positions have been saved every 500 steps (i.e., 1.0 ps) for the analyses. The simulation time chosen is fully suitable to accurately organize and stabilize the new modeled protein-protein interfaces.

## Analyses

Root mean square deviations (RMSD), root mean square fluctuations (RMSF), radius of gyration (Rg), time dependence of the hydrogen-bond persistence and the secondary structure evolution were obtained using the GROMACS MD package version 4.5.5 [37]. Salt bridges analysis was carried out through the VMD [38] salt-bridges plug-in (see the Supplementary material).

A correct assembling is justified only if acceptable interfaces are formed. To verify the reliability of the models interfaces, i.e., if they are on average as observed in the known proteins structures, the PDBePISA web server (http://www.ebi.ac.uk/msd-srv/prot_int/pistart.html) [39] has been used. PDBePISA is an interactive tool for the exploration of macromolecular interfaces able to assess the biological role of interfaces on the basis of structural and chemical properties of interfacing residues (hydrogen bonds, disulfide bridges, salt bridges, hydrophobicity, hydrophilicity). After the interface analysis PDBePISA [39] returns an index value named CSS. CSS stands for the complexation significance score, which indicates how significant for assembly formation the interface is. CSS ranges from 0 to 1 as interface relevance to complexation increases. Achieved CSS values greater than or equal to 0.5 implies that the interface plays an essential role in complexation. The score is defined as a maximal fraction of the total free energy of binding that belongs to the interface in

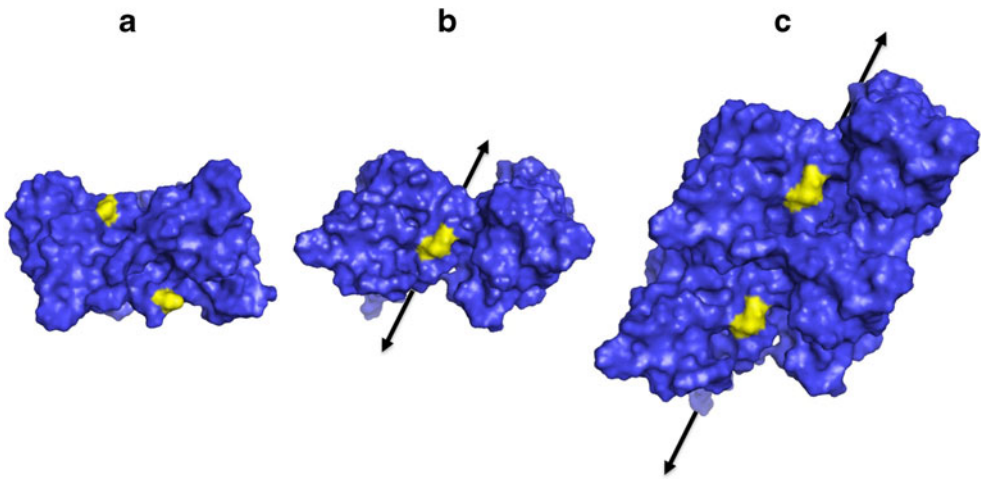


**Fig. 3** Solid solvent accessible surface representations of: (**a**) the standard SOD1 dimer; (**b**) the inter-subunit disulfide linked SOD1 dimer and (**c**) the ALS-linked SOD1 dimer of dimers. The *yellow* spot on the surface indicates the Cys57-Cys57 inter-chain disulfide bridge. The *black double head arrows* show the elongation axis of the fibril. The PyMOL [43] (http://www.pymol.org) program has been used to make this picture

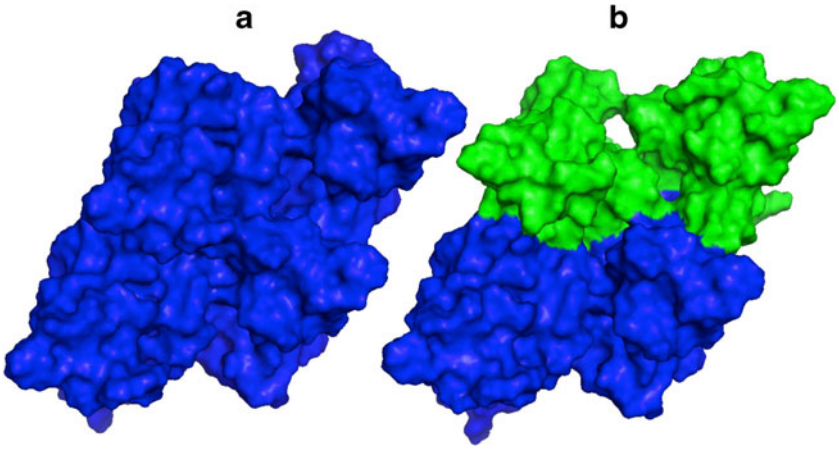


**Fig. 4** **a** Solvent accessible surface representation of the ALS-linked SOD1 dimer of dimers. **b** Solvent accessible surface representation of the hybrid ALS-linked SOD1 assembly. The inter-subunits disulfide linked dimers are represented by a *blue surface* while the intra-subunit disulfide monomers are indicated by a *green surface*. The PyMOL [43] (http://www.pymol.org) program has been used to make this picture

stable assemblies [39]. The protein-protein docking analysis between the dimers of dimers has been carried out using the PatchDock [40] web server (http://bioinfo3d.cs.tau.ac.il/PatchDock/).

## Results and discussions

### Packing of SOD1 subunits

#### *Disulfide linked dimer*

The model of the novel SOD1 dimer (Fig. 3b), suggested as potential nucleation site of the ALS fibril, has been built starting from the NMR structure of the reduced intra-subunit disulfide bridge and copper-free SOD1 [24]. This structure is characterized by a high mobility of the larger SOD1 loop (loop 6,5) due to the loss of the disulfide covalent anchor to the β-barrel. In the structure some hydrophobic residues, that in Cu,Zn SOD1 are located toward the β-barrel, are exposed toward the exterior. The high mobility of loop 6,5 permits a high degree of freedom to Cys57 that, due to a translation of one monomer, can face the Cys57 of the second monomer to form an inter-subunit disulfide bridge. The zinc ion has been left in the structure because, as experimentally observed, its presence allows the ALS fibril nucleation and elongation [14].

#### *Dimers of dimers*

The inter-subunits disulfide linked dimer exposes to the solvent the original hydrophobic surface that stabilizes the native SOD1 dimer (Fig. 3a). A new dimer of dimers (Fig. 3c) can then be easily formed through the interaction of this large hydrophobic surface flanked by salt bridges and hydrogen bonds.

To evaluate if, as experimentally observed, the elongation of the ALS fibril could also involve apo-Cu monomers with intact

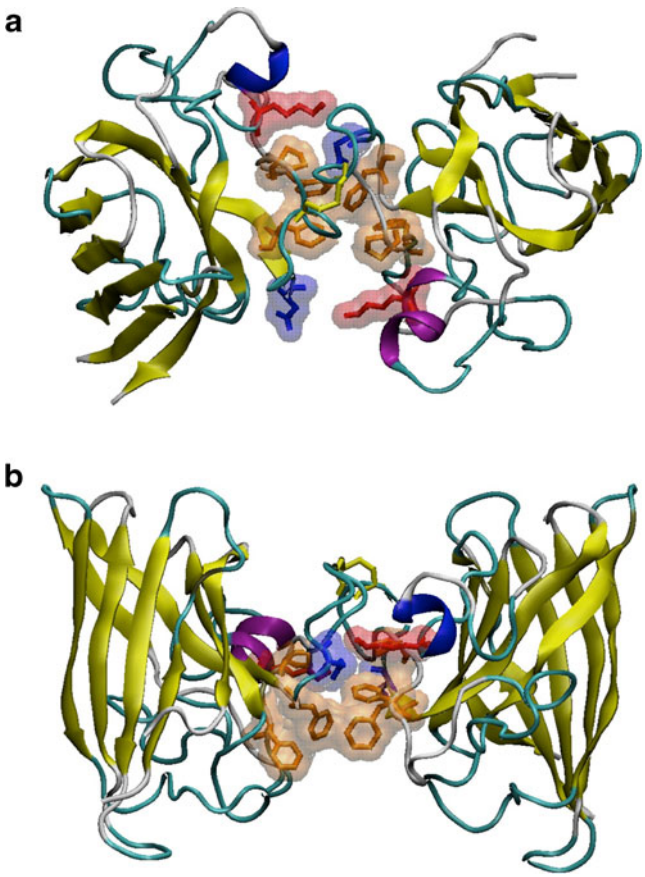


**Fig. 5** The new interface of the disulfide linked SOD1 dimer. The *yellow arrows* indicate the β-strands while the *blue* and *violet ribbons* show the short helices in loop 6,5. **a** View of the interface along the two-fold symmetry axis. **b** View of the interface perpendicular to the two-fold symmetry axis. The disulfide bridge is indicated by the *yellow wire* representation, the aromatic/hydrophobic interactions (involving residues Phe50, Phe64 and Pro62) are shown by the *orange* residues behind the disulfide bridge while the salt bridges (involving residues Asp52 and Lys136 of both subunits) are represented by the *red* (positively charged) and *blue* (negatively charged) residues. The VMD [38] (http://www.ks.uiuc.edu/Research/vmd/) program has been used to make this picture

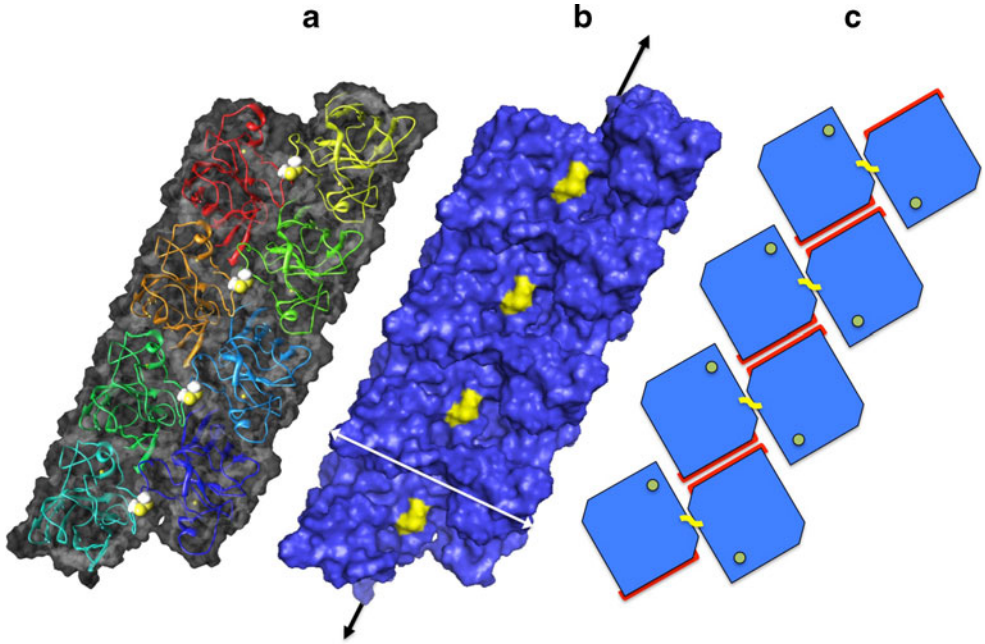


**Fig. 6** **a** Solvent accessible surface representation of the ALS-linked SOD1 tetramer of dimers. Inside the surface the different monomer chains are indicated by different colors. The spacefill representation indicates the Cys57 disulfide bridges while the small *green* sphere represents the zinc ion. **b** *Blue* solid solvent accessible surface representations of SOD1 tetramer of dimers. The *yellow* spot on the surface indicates the Cys57-Cys57 inter-chain disulfide bridge. The *white double head arrow* shows the width of the fibril (about 6 nm), while the *black double head arrows* show the elongation axis of the fibril. **c** Schematic representation of the ALS-linked tetramer of dimers. The UCSF Chimera [45] (www.cgl.ucsf.edu/chimera), and the PyMOL [44] (http://www.pymol.org) programs have been used to make this picture

intra-subunit disulfide bridge [14], a hybrid assembly has been also modeled utilizing one inter-subunits disulfide linked dimer and two apo-Cu monomers with the intact intra-subunit disulfide bridge [25].

Also the hybrid dimer of dimers shows favorable hydrophobic contacts, established through the original inter-subunit surface, and about the same number of salt bridges and hydrogen bonds interactions found in the dimer of dimers stabilizes the novel extended interface. The hybrid dimer of dimers has then an interface similar to that of the disulfide linked dimer of dimers (Fig. 4a), although the lack of the Cys57 inter-subunit disulfide bridge initially generates a cavity (Fig. 4b) that is largely reduced after the MD refinement (see the Supplementary material).

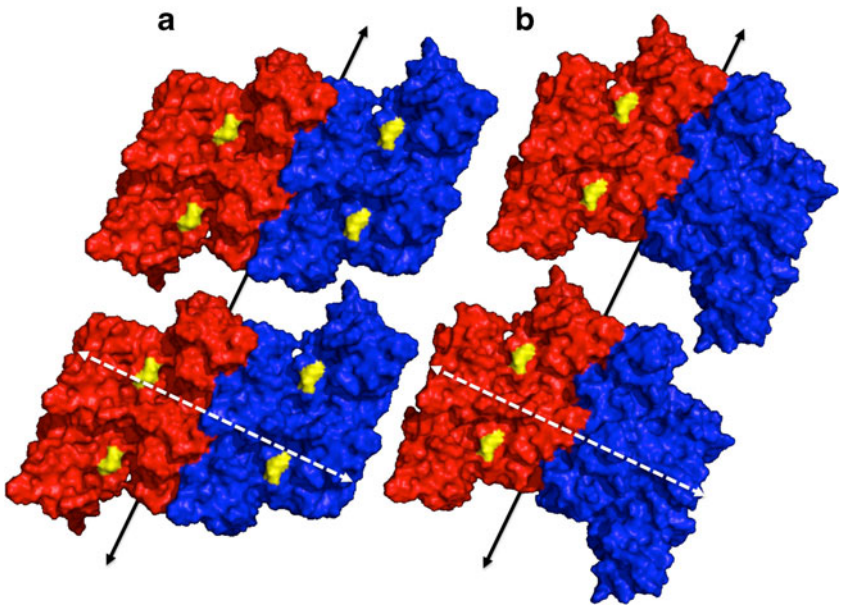


**Fig. 7** Two representative dimers of dimers complexes compatible with a fibril width of 12–15 nm. The dimers of dimers are represented by the *red* and *blue* solid solvent accessible surfaces while the *yellow* spot on the surface indicates the Cys57-Cys57 inter-chain disulfide bridge. **a** Parallel dimers of dimers assembly and (**b**) anti-parallel dimers of dimers assembly. The *white dotted double head arrow* shows the width axis of the fibril (about 12 nm), while the *black double head arrows* the length elongation axis of the fibril. The PyMOL [44] (http://www.pymol.org) program has been used to make this picture

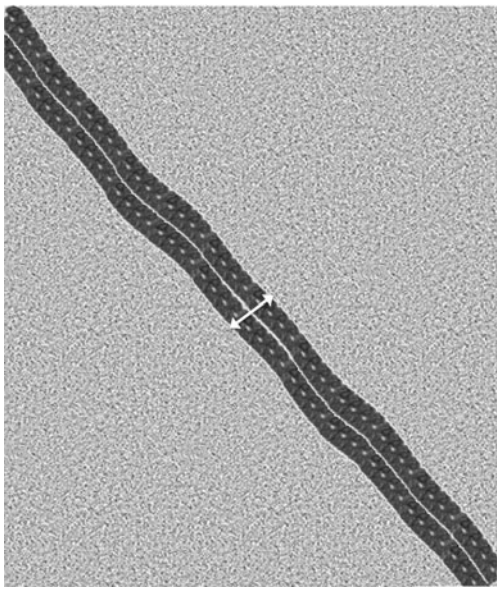

**Fig. 8** Graphic representation of an electron microscopy image showing the hypothetic modeled fibril composed of two narrow strands. The *white double head arrow* shows the width of the coupled narrow strands (about 12 nm). The PyMOL [44] (http://www.pymol.org) program has been used to make this picture

## Interfaces description

### *Wildtype dimer*

In the standard human SOD1 the contact surface across the dimer two-fold axis is closely fitted and extensive [41]. Analysis through the PDBePISA [39] web server reveals that about 680 Å$^2$ are buried in the contact and the interface is composed of 41 residues participating in the contact between the two monomers with 150 atoms. Six hydrogen bonds contribute to the stabilization of this interface. The interactions involve the N and C termini, the first and last pair of β-strands of the β-barrel and two loop regions [24]. The PDBePISA CSS score returned for this structure is 1.0.

### *Disulfide linked dimer*

The new interface modeled in the SOD1 disulfide linked dimer, mainly composed of loop 6,5, has a starting extension of about 526 Å$^2$ and it is composed of 29 residues that participates in the contact between the subunits with 108 atoms.

The new interface is stabilized by the inter-chain disulfide bridge between the Cys57 of the two monomers and by an aromatic/hydrophobic cluster between Phe50, Phe64 and Pro62 of the two monomers that lies below the inter-chain disulfide bridge (Fig. 5a, b) and by the presence of two hydrogen bonds. The PDBePISA web server [39] CSS score returned for the initial model is about 0.2, which indicates that the initial characteristics of the interface are not very significant for the assembly formation. After 10 ns of MD simulation, carried out to refine the interface, PDBePISA [39] returned the maximum CSS score of 1.0, indicating that after the regularization of the model the interface is very relevant in complex stabilization and formation. The final interface extension is about 508 Å$^2$ and, although less extended than the initial, is well packed and composed of 30 residues, interacting through 102 atoms. The refined interface is stabilized by three hydrogen bonds and by two symmetric salt bridges, between Asp52 and Lys136 of the two monomers, located at the border of the aromatic/hydrophobic interaction.

### *Dimer of dimers*

The interface in the dimer of dimers, composed of disulfide linked SOD1 dimers, is about 2290 Å$^2$ wide and it is initially composed of 130 residues that participate in the contact between the dimers through 478 atoms. The interface between two dimers includes, at its center, the interface of the standard SOD1 dimer but is extended and flanked by close interactions between a part of loop 6,5 and β-strands 1 to 4, which form the more regular side of the SOD1 barrel. The PDBePISA web server [39] CSS score returned for the initial model is 0.0, indicating that the initial interface assembly is not relevant for the complex formation. MD simulation of dimer of dimers also lead to a large refinement of the structure. In this case, after 10 ns of MD simulation, carried out to refine the interface, a reorganization of the inter-dimers hydrogen bonds and salt bridges network has been observed, leading to a large stabilization of the new interface. The new interface, with an extension of about 1800 Å$^2$, is composed of 105 residues, participating with 362 atoms to the contact between the two dimers. This large and curved interface is mainly stabilized by hydrophobic interactions between the two dimers due to a large number of hydrophobic contacts between several residues, by 11 long-time persistent hydrogen bonds and by the presence of seven salt bridges. The final model, submitted to PDBePISA [39], obtained the maximum CSS score of 1.0.

### *Hybrid dimer of dimers*

The starting interface in the hybrid dimer of dimers, composed of one disulfide linked SOD1 dimer and two apo-Cu, intra-subunit disulfide SOD1 monomers, is about 2220 Å$^2$ wide and it is composed of 119 residues that participate in the contact between the dimers through 521 atoms. Also in this case the PDBePISA web server [39] CSS score returned for the initial model is 0, but as previously observed in the dimers of dimers, 10 ns MD simulation, carried out to refine the interface, leads to a rearrangement of the interface residues, hydrogen bonds and salt bridges network. The final

interface is extended for about 1900 Å$^2$, composed of 114 residues participating in the contact through 432 atoms and, as observed for the dimer of dimers, is stabilized by a large number of hydrophobic contacts in the inner region, by 16 long-time persistent hydrogen bonds and by eight salt bridges. The final model, submitted to PDBePISA [39], received the maximum CSS score of 1.0, suggesting that also the hybrid dimer of dimers could have a role in the aggregation [42].

*Fibril elongation and coupling*

As a first step of the ALS fibril elongation the disulfide linked dimer of dimers has been once more duplicated to obtain a tetramer of dimers (Fig. 6a, b, c). In this case the interface, described in the dimer of dimers formation, can be reused to generate very stable and longer assemblies that can infinitely propagate to create a long narrow strand along the elongation axis defined by the black arrow in Fig. 6.

In order to evaluate the single narrow strand propensity to couple and to generate the large fibril composed of two or four narrow strands, a docking investigation between two dimers of dimers, in the direction perpendicular to the elongation axis, has been carried out using the PatchDock [40] web server (http://bioinfo3d.cs.tau.ac.il/PatchDock/). The docking procedure identifies 1256 complexes. Analysis of the first 100 best complexes indicates that two dimers of dimers can stack, one over the other, exploring different structural arrangements stabilized by hydrophobic and electrostatic interactions that occur between deep surface furrows and high crests. Among the checked solutions, nine give rise to stable interactions that provide complexes with the experimentally reported width of about 12 nm [14, 16]. The interaction between two narrow strands can be both parallel (Fig. 7a) or anti-parallel (Fig. 7b).

In the case of the parallel interaction, PDBePISA [39] results indicate that the lateral interface, that doubles the fibril width, is about 1950 Å$^2$ wide and it is composed of 123 residues that participate in the contact between the dimers of dimers with 482 atoms. The interface is stabilized by hydrophobic interactions, three salt bridges and eight hydrogen bonds. In the case of the anti-parallel interaction the lateral interface, that doubles the fibril width, is about 1900 Å$^2$ wide and includes 135 residues participating in the contacts with 480 atoms. The interface is stabilized by hydrophobic interactions, eight salt bridges and four hydrogen bonds. Both the assemblies show the necessary complementarity to build the experimentally observed two or four narrow-strand fibrils [14, 16].

In the electron micrographs images [14, 16] the SOD1 fibril has a diameter of about 12–15 nm and apparently consists of two narrower strands loosely wound together. Fibrils can also associate in pairs that are aligned or loosely twisted together to form thicker fibrils with net diameter of about 25 nm (four narrow strands) [14, 16]. The ALS fibril model here proposed, when measured perpendicularly to the fibril elongation axis (Fig. 8), shows a width of about 6 nm consistent with the experimentally observed narrow strand that, associating with an identical strand, generates the 12 nm fibril [14, 16] (Fig. 8).

## Conclusions

The structural model shown here (Fig. 3b) represents a rational hypothesis, based on experimental data [14, 16] and results obtained by previous structural simulations [21–23], explaining the nucleation and the elongation strategy (Figs. 3c and 6a, b, c) of SOD1 ALS-linked fibrils that play a role in the pathogenesis interfering with the physiological function of motor-neurons.

The inter-chain disulfide bridge that covalently links the ALS-linked SOD1 subunits [14] is structurally achievable only when the large loop 6,5 of SOD1, in the absence of copper and of the intra-chain disulfide bridge (Cys57-Cys146), becomes unstable exposing Cys57 and some hydrophobic residues, normally leaning on the β-barrel surface, become a "sticky" hydrophobic patch that permits the formation of a new inter-subunits surface. In the meantime the specific interface, that normally ensures the dimeric interaction in SOD1, becomes available for inter-dimeric interactions.

The packing motifs proposed here give explanation for the observed SOD1 fibrillation and obey the rules for the aggregation of proteins in which the exposure of sticky surfaces due to a structure destabilization promotes the nucleation and the absence of repulsive charges increases the rate of aggregation [20, 43]. Our structural model, fully consistent with the fibril dimensions observed through electron micrography [14, 16] (Figs. 7a,b and 8), provides the molecular scaffold to propose experiments able to confirm this assemblage that, once validated, will makes possible the design of devices able to prevent the nucleation and growth of ALS-linked fibrils.

## References

1. Haverkamp LJ, Appel V, Appel SH (1995) Natural history of amyotrphic lateral sclerosis in a database population. Validation of scoring system and a model for survival prediction. Brain 118:707–719
2. Deng HX, Hentati A, Tainer JA, Iqbal Z, Cayabyab A, Hung WY, Getzoff ED, Hu P, Herzfeldt B, Roos RP, Warner C, Deng G, Soriano E, Smyth C, Parge HE, Ahmed A, Roses AD, Hallewell RA, Pericak-Vance MA, Siddique T (1993) Amyotrophic lateral sclerosis and structural defects in Cu,Zn superoxide dismutase. Science 261:1047–1051

3. Rosen DR (1993) Mutations in Cu/Zn superoxide dismutase gene are associated with familial amyotrophic lateral sclerosis. Nature 362:59–62
4. Valentine JS, Doucette PA, Potter SZ (2005) Copper-zinc superoxide dismutase and amyotrophic lateral sclerosis. Annu Rev Biochem 74:563–593
5. Tiwari A, Hayward LJ (2003) Familial amyotrophic lateral sclerosis mutants of copper/zinc superoxide dismutase are susceptible to disulfide reduction. J Biol Chem 278:5984–5992
6. Bruijn LI, Miller TM, Cleveland DW (2004) Unraveling the mechanisms involved in motor neuron degeneration in ALS. Annu Rev Neurosci 27:723–749
7. Bruening W, Roy J, Giasson B, Figlewicz DA, Mushynski WE, Durham HD (1999) Up-regulation of protein chaperones preserves viability of cells expressing toxic Cu/Zn-superoxide dismutase mutants associated with amyotrophic lateral sclerosis. J Neurochem 72:693–699
8. Okado-Matsumoto A, Fridovich I (2002) Amyotrophic lateral sclerosis: a proposed mechanism. Proc Natl Acad Sci USA 99:9010–9014
9. Borchelt DR, Wong PC, Becher MW, Pardo CA, Lee MK, Xu ZS, Thinakaran G, Jenkins NA, Copeland NG, Sisodia SS, Cleveland DW, Price DL, Hoffman PN (1998) Axonal transport of mutant superoxide dismutase 1 and focal axonal abnormalities in the proximal axons of transgenic mice. Neurobiol Dis 5:27–35
10. Williamson TL, Cleveland DW (1999) Slowing of axonal transport is a very early event in the toxicity of ALS-linked SOD1 mutants to motor neurons. Nat Neurosci 2:50–56
11. Johnston JA, Dalton MJ, Gurney ME, Kopito RR (2000) Formation of high molecular weight complexes of mutant Cu, Zn-superoxide dismutase in a mouse model for familial amyotrophic lateral sclerosis. Proc Natl Acad Sci USA 97:12571–12576
12. Kato S, Hayashi H, Nakashima K, Nanba E, Kato M, Hirano A, Nakano I, Asayama K, Ohama E (1997) Pathological characterization of astrocytic hyaline inclusions in familial amyotrophic lateral sclerosis. Am J Pathol 151:611–620
13. Shibata N, Hirano A, Kobayashi M, Sasaki S, Kato T, Matsumoto S, Shiozawa Z, Komori T, Ikemoto A, Umahara T, Asayama K (1994) Cu/Zn superoxide dismutase-like immunoreactivity in Lewy bodylike inclusions of sporadic amyotrophic lateral sclerosis. Neurosci Lett 179:149–152
14. Chattopadhyay M, Durazo A, Sohn SH, Strong CD, Gralla EB, Whitelegge JP, Valentine JS (2008) Initiation and elongation in fibrillation of ALS-linked superoxide dismutase. Proc Natl Acad Sci USA 105:18649–18650
15. Di Donato M, Craig L, Huff ME, Thayer MM, Cardoso RM, Kassmann CJ, Lo TP, Bruns CK, Powers ET, Kelly JW, Getzoff ED, Tainer JA (2003) ALS mutants of human superoxide dismutase form fibrous aggregates via framework destabilization. J Mol Biol 332:601–615
16. Stathopulos PB, Rumfeldt JA, Scholz GA, Irani RA, Frey HE, Hallewell RA, Lepock JR, Meiering EM (2003) Cu/Zn superoxide dismutase mutants associated with amyotrophic lateral sclerosis show enhanced formation of aggregates in vitro. Proc Natl Acad Sci USA 100:7021–7026
17. Furukawa Y, Kaneko K, Yamanaka K, O'Halloran TV, Nukina N (2008) Complete loss of post-translational modifications triggers fibrillar aggregation of SOD1 in familial form of ALS. J Biol Chem 283:24167–24176
18. Seetharaman SV, Prudencio M, Karch C, Holloway SP, Borchelt DR, Hart PJ (2009) Immature copper-zinc superoxide dismutase and familial amyotrophic lateral sclerosis. Exp Biol Med 234:1140–1154
19. Sheng Y, Chattopadhyay M, Whitelegge J, Valentine JS (2012) SOD1 Aggregation and ALS: role of metallation states and disulfide status. Curr Top Med Chem 12:2560–2572
20. Mulligan VK, Chakrabartty A (2013) Protein misfolding in the late-onset neurodegenerative diseases: common themes and the unique case of amyotrophic lateral sclerosis. Proteins doi:10.1002/prot.24285
21. Strange RW, Yong CW, Smith W, Hasnain SS (2007) Molecular dynamics using atomic-resolution structure reveal structural fluctuations that may lead to polymerization of human Cu-Zn superoxide dismutase. Proc Natl Acad Sci U S A 104:10040–10044
22. Ding F, Dokholyan NV (2008) Dynamical roles of metal ions and the disulfide bond in Cu, Zn superoxide dismutase folding and aggregation. Proc Natl Acad Sci U S A 105:19696–19701
23. Ding F, Furukawa Y, Nukina N, Dokholyan NV (2012) Local unfolding of Cu, Zn superoxide dismutase monomer determines the morphology of fibrillar aggregates. J Mol Biol 421:548–560
24. Banci L, Bertini I, Cantini F, D'Amelio N, Gaggelli E (2006) Human SOD1 before harboring the catalytic metal: solution structure of copper-depleted, disulfide-reduced form. J Biol Chem 281:2333–2337
25. Strange RW, Antonyuk S, Hough MA, Doucette PA, Rodriguez JA, Hart PJ, Hayward LJ, Valentine JS, Hasnain SS (2003) The structure of holo and metal-deficient wild-type human Cu, Zn superoxide dismutase and its relevance to familial amyotrophic lateral sclerosis. J Mol Biol 328:877–891
26. Case DA, Cheatham TE III, Darden T, Gohlke H, Luo R, Merz KM Jr, Onufriev A, Simmerling C, Wang B, Woods R (2005) The Amber biomolecular simulation programs. J Comput Chem 26:1668–1688
27. Duan Y, Wu C, Chowdhury S, Lee MC, Xiong G, Zhang W, Yang R, Cieplak P, Luo R, Lee T, Caldwell J, Wang J, Kollman P (2003) A point-charge force field for molecular mechanics simulations of proteins based on condensed-phase quantum mechanical calculations. J Comput Chem 24:1999–2012
28. Pang YP (1999) Novel zinc protein molecular dynamics simulations: steps toward antiangiogenesis for cancer treatment. J Mol Model 5:196–202
29. Falconi M, Oteri F, Di Palma F, Pandey S, Battistoni A, Desideri A (2011) Structural-dynamical investigation of the ZnuA histidine-rich loop: involvement in zinc management and transport. J Comput Aided Mol Des 225:181–94
30. Jorgensen WL, Chandrasekhar J, Madura JD, Impey RW, Klein ML (1983) Comparison of simple potential functions for simulating liquid water. J Chem Phys 79:926
31. Darden T, York D, Pedersen L (1993) Particle mesd Ewald: an $N\cdot\log(N)$ method for Ewald sums in large systems. J Chem Phys 98:10089
32. Ryckaert JP, Ciccotti G, Berendsen HJC (1977) Numerical integration of the Cartesian equations of motion of a system with constraints: molecular dynamics of n-alkanes. J Comp Phys 23:327–341
33. Miyamoto S, Kollman PA (1992) Settle: an analytical version of the SHAKE and RATTLE algorithm for rigid water models. J Comput Chem 13:952–962
34. Loncharich RJ, Brooks BR, Pastor RW (1992) Langevin dynamics of peptides: the frictional dependence of isomerization rates of *N*-acetylalanyl-*N*′-methylamide. Byopolymers 32:523–535
35. Feller SE, Zhang Y, Pastor RW, Brooks BR (1995) Constant pressure molecular dynamics simulation: the Langevin piston method. J Chem Phys 103:4613
36. Phillips JC, Braun R, Wang W, Gumbart J, Tajkhorshid E, Villa E, Chipot C, Skeel RD, Kale L, Schulten K (2005) Scalable molecular dynamics with NAMD. J Comput Chem 26:1781–1802
37. Hess B, Kutzner C, van der Spoel D, Lindahl E (2008) GROMACS 4: algorithms for highly efficient, load-balanced, and scalable molecular simulation. J Chem Theory Comput 4:435–447
38. Humphrey W, Dalke A, Schulten K (1996) VMD - Visual Molecular Dynamics. J Mol Graph 14:33–38
39. Krissinel E, Henrick K (2007) Inference of macromolecular assemblies from crystalline state. J Mol Biol 372:774–797

40. Schneidman-Duhovny D, Inbar Y, Nussinov R, Wolfson HJ (2005) PatchDock and SymmDock: servers for rigid and symmetric docking. Nucl Acids Res 33:363–367
41. Tainer JA, Getzoff ED, Beem KM, Richardson JS, Richardson DC (1982) Determination and analysis of the 2 Å structure of copper, zinc superoxide dismutase. J Mol Biol 160:181–217
42. Roberts BLT, Patel K, Brown HH, Borchelt DR (2012) Role of disulfide cross-linking of mutant SOD1 in the formation of inclusion-body-like structures. PLoS One 7:e47838
43. Rousseau F, Serrano L, Schymkowitz JW (2006) How evolutionary pressure against protein aggregation shaped chaperone specificity. J Mol Biol 355:1037–1047
44. DeLano WL (2002) The PyMOL Molecular Graphics System World Wide Web (http://www.pymol.org)
45. Pettersen EF, Goddard TD, Huang CC, Couch GS, Greenblatt DM, Meng EC, Ferrin TE (2004) UCSF Chimera - a visualization system for exploratory research and analysis. J Comput Chem 25:1605–1612